ACS Photonics

Article

Cite This: ACS Photonics XXXX, XXX, XXX−XXX

pubs.acs.org/journal/apchd5

Ultra-Low Power Light Emission via Avalanche and Sub-avalanche Breakdown in Suspended Carbon Nanotubes

Bo Wang,[†] Sisi Yang,[†] Lang Shen,[§] and Stephen B. Cronin*[,†,‡]

[†]Department of Physics and Astronomy, [‡]Ming Hsieh Department of Electrical Engineering, and [§]Mork Family Department of Chemical Engineering and Materials Science, University of Southern California, Los Angeles, California 90089, United States

Supporting Information

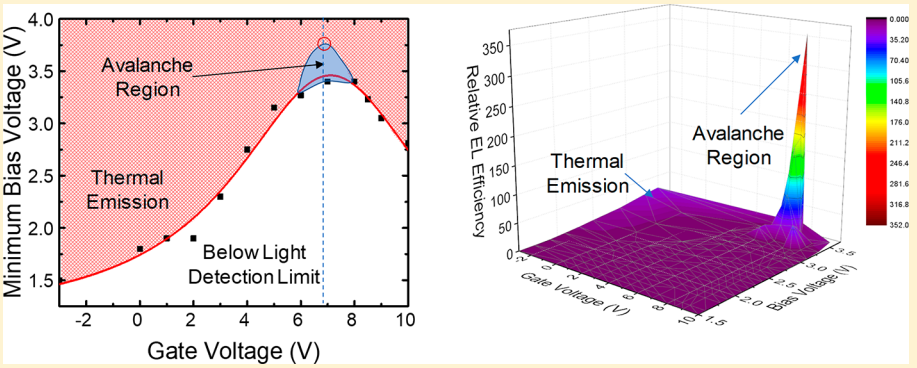

ABSTRACT: We explore near-infrared light emission in suspended carbon nanotube field effect transistors over a wide range of gate and bias voltages. An abrupt increase in both the electric current (90 μA/V) and electroluminescence intensity is observed at high bias voltages (~3.5 V), when gated in the "off" state (i.e., $V_{gate} > 0$ V). For bias voltages below the threshold for avalanche breakdown, we observe light emission due to the creation of exitons by impact ionization under these high electric fields. Here, we find that there is a relatively small region over which low power (~nW) light emission is observed. By plotting the relative luminescence efficiency (i.e., light intensity/electrical power) as a function of the gate and bias voltages, we observe a very sharp feature corresponding to avalanche emission at which the electroluminescence efficiency is 2−3 orders of magnitude higher than that under all other conditions of gate and bias voltage. A steep increase in the current with bias voltage (i.e., large dI/dV_b) is observed at the same gate and bias conditions of the highly efficient electroluminescence and signifies the onset of the avalanche process. We believe that these results demonstrate additional mechanistic evidence for achieving highly efficient light emission in carbon nanotubes via avalanche breakdown.

KEYWORDS: *ballistic, avalanche, high-field, band-to-band, photoemission*

Recent research of light emission from nanoscale systems, such as carbon nanotubes (CNTs) and III−V semiconducting quantum dots, shows several interesting optical and optoelectronic phenomena including exciton and trion formation and room-temperature single photon emission (SPE) at telecommunications wavelengths (1300−1550 nm).[1−5] High purity single photon sources (SPSs) are a key component needed for quantum information and computing technologies. Electroluminescence (EL) from substrate-supported single CNT pn-junction devices was first demonstrated by the IBM group in 2003.[6,7] They reported a light emission efficiency around 10^{-4} photons per injected electron−hole pair. In addition to these pn-junction devices, several CNT FET-based devices (FET = field effect transistor) exhibiting electroluminescence have also been reported from several groups.[8−11] In these previous single nanotube studies, an empirical threshold of 1 μW of applied electrical power was required in order to detect light emission from these CNT FET devices. At these applied powers, however, substantial Joule heating occurs, which can be monitored by the G-band shift in their Raman spectra.[12] As a result, thermal emission caused by heating is likely the main mechanism of light emission occurring in these previous works. In order to develop electrically driven single photon emitters based on carbon nanotubes for quantum communication, it is absolutely essential that highly efficient electroluminescent carbon nanotube devices be demonstrated.

Photoluminescence from carbon nanotubes was first observed in 2002 by O'Connell et al.,[13] which was followed by many further optical and optoelectronic studies of CNTs. Lefebrve et al. reported bright photoluminescence from suspended regions of carbon nanotubes, which indicated that suspended CNTs had a much higher luminescence efficiency than substrate-supported CNTs.[14] In 2005, Chen et al. observed bright electroluminescence from partly suspended

Received: July 3, 2018
Published: October 16, 2018

DOI: 10.1021/acsphotonics.8b00896
ACS Photonics XXXX, XXX, XXX−XXX

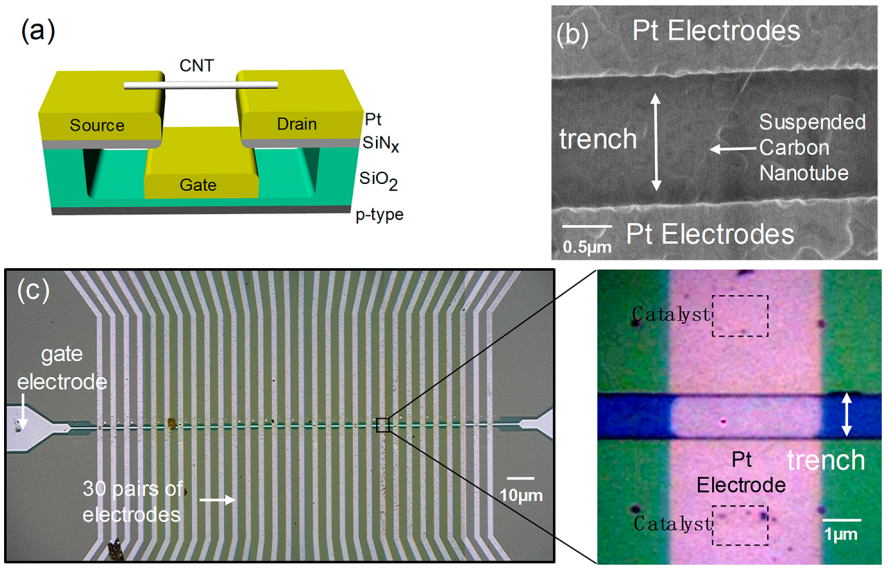

Figure 1. (a) Schematic diagram, (b) scanning electron microscope (SEM) image, and (c) optical microscope images of a suspended carbon nanotube field effect transistor.

carbon nanotubes, which they attributed to the high fields produced at the region between the suspended and non-suspended parts of CNT that provide enough electrical energy for exciton creation and subsequent light emission.[15] Khasminskaya et al. observed electrically driven single photon emission from a CNT-based photonic circuit under cryogenic conditions in 2016.[16] In 2017, He et al. showed that, by introducing aryl sp^3 defects in single-walled CNTs through a solution-based doping method, they can achieve single photon emission with a low probability of multiphoton emission at room temperature.[5] Electroluminescence with various of approaches are also reported by many other groups.[17−22] Most recently, Wang et al. reported avalanche emission in CNT FETs under extremely high electric fields (0.5 MV/cm).[12] Here, the drive currents were 3 orders of magnitude lower, while the EL efficiencies were 3 orders of magnitude higher, than previous reports in the literature, and Raman spectroscopy was used to explicitly rule out thermal emission.[8,10,23,11,23] While several demonstrative measurements were shown, this previous report did not study this effect over a wide range of gate voltage conditions, nor did it present a consistent picture of electron transport and EL emission.

In the work presented here, we have systematically explored light emission in these suspended CNT FET devices over a wide range of experimental device parameters (i.e., gate voltage, bias voltage, bias current, and light intensity), in order to further establish and understand the origin of this avalanche emission mechanism. Here, we are able to tune through various mechanisms of light emission from thermal emission to avalanche electroluminescence. By comparing the bias voltage dependence of the electric current and EL intensity, we observe a region under which sub-avalanche light emission is observed. There appears to be a "sweet spot" in gate voltage at which the avalanche emission process occurs. Here, the current−voltage characteristics of each device were used to verify that they consist of individual nanotubes rather than multiple nanotubes. On the basis of several years of measurements involving these devices, we have found that individual, suspended nanotube devices exhibit negative differential conductance above approximately 1.2 V with a maximum current of 3−5 μA.[24−26] A plot of the current vs bias voltage showing NDC can be found in the Supporting Information document.

Figure 1a shows a schematic diagram of the CNT FET device. In the device fabrication process, a 1 μm wide trench is etched in a $Si/SiO_2/Si_3N_4$ wafer approximately 500 nm deep. Thirty pairs of platinum source and drain electrodes are then patterned on the surface of the wafer along with one common gate electrode on the bottom of the trench using photolithography. A scanning electron microscope (SEM) image of a CNT suspended over the trench is shown in Figure 1b. Figure 1c shows optical microscope images of a typical chip,[27−29] indicating the approximate size of the device. Lithographically defined windows are introduced into a photoresist layer on the source and drain electrodes for the controlled deposition of ferric nitrate ($Fe(NO_3)_3$) catalyst. To avoid chemical contamination by the lithographic processes, the last step of the sample fabrication is CNT growth by chemical vapor deposition (CVD) at 825 °C using hydrogen and argon gas, which is passed through pure ethanol.[30] A semiconductor parameter analyzer is used for the electrical characterization of these devices. During these measurements, the drain electrode is grounded and all the values of gate and bias voltage are applied with respect to the drain electrode. Electroluminescence images are collected with a thermoelectrically cooled InGaAs camera (Xenics, Inc.) with an effective wavelength range from 1000 to 1600 nm. This IR camera is capable of outputting the light intensity for selected regions or individual pixels in the EL image.

Figure 2 shows semi-log plots of the electric current and the electroluminescence intensity plotted as a function of applied bias voltage at a gate potential of V_g = +7 V. In Figure 2a, there is a very steep jump in the current with a very large differential conductance of 90 μA/V, which indicates the onset of the avalanche breakdown of V_{bias} = 3.75 V. In Figure 2b, we observe the onset of electroluminescence at V_{bias} = 3.4 V, which is 0.35 V below the threshold for avalanche breakdown, as observed in the current−bias voltage data. Here, in the "sub-avalanche" regime (between V_{bias} = 3.4 and 3.8 V), ballistic electrons accelerating in the high electric fields gain enough

DOI: 10.1021/acsphotonics.8b00896
ACS Photonics XXXX, XXX, XXX−XXX

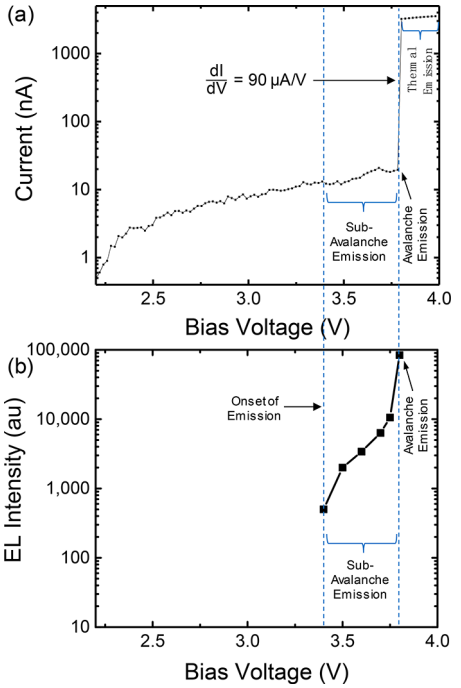

Figure 2. Semi-log plots of (a) the electric current and (b) EL intensity plotted as a function of applied bias voltage at a gate potential of V_g = +7 V. The value of the maximum differential conductance is labeled in the plot (a).

kinetic energy for an exciton decay (~0.8 eV), resulting in light emission. The electric field required to separate these excitons into free electron−hole pairs is substantially high ($E \approx$ exciton binding energy/exciton size ≈ 0.8 MV/cm). This threshold for exciton separation and subsequent carrier multiplication can be seen by the abrupt increase in current at V_{bias} = 3.75 V. It should be noted that the differential conductance associated with the avalanche process is so steep that the device reaches the thermal emission regime extremely quickly, as labeled in this plot. This occurs when the current reaches the μA range, and thus the voltage range over which avalanche emission is the dominant mechanism of light emission is actually quite small compared with thermal emission, as discussed in the following paragraph.

Figure 3a shows the minimum bias voltage needed to reach the light detection limit of our experimental setup plotted as a function of the gate voltage for the same CNT FET device shown in Figure 2. We also measured the current and EL intensity as a function of bias voltage at different gate voltages. We measured the current and EL intensity as a function of bias voltage at different gate voltages. By monitoring the light emission as a function of current, we are able to find the bias voltage at which avalanche and sub-avalanche light emission occurs at each value of gate voltage and then we connected these points to get the triangular region. Here, we see that there is a relatively small "triangular" region over which low power avalanche and sub-avalanche emission is observed, with a current of less than 5 nA and an electrical power less than 20 nW, which are both well below the threshold current and power for thermal emission.[8,10,23,11,23] Outside this "triangular" region and above the solid curve, which is shaded in this plot, the electrical power is always larger than several μW and the CNT exhibits thermal emission under these conditions. Figure 3b shows a 3D plot of the relative electroluminescence efficiency (i.e., light intensity/electrical power) plotted as a function of the gate and bias voltages, in which there is a sharp feature corresponding to avalanche emission. Figure 3c shows a plot of the maximum differential conductance (MaxDC) under different values of the applied gate voltage, which is caused by the carrier multiplication in the avalanche process. Here, the peak in the MaxDC occurs at the same gate voltage as the avalanche emission and highest EL efficiency. These data sets show that there appears to be a "sweet" spot around V_g = +7 V,

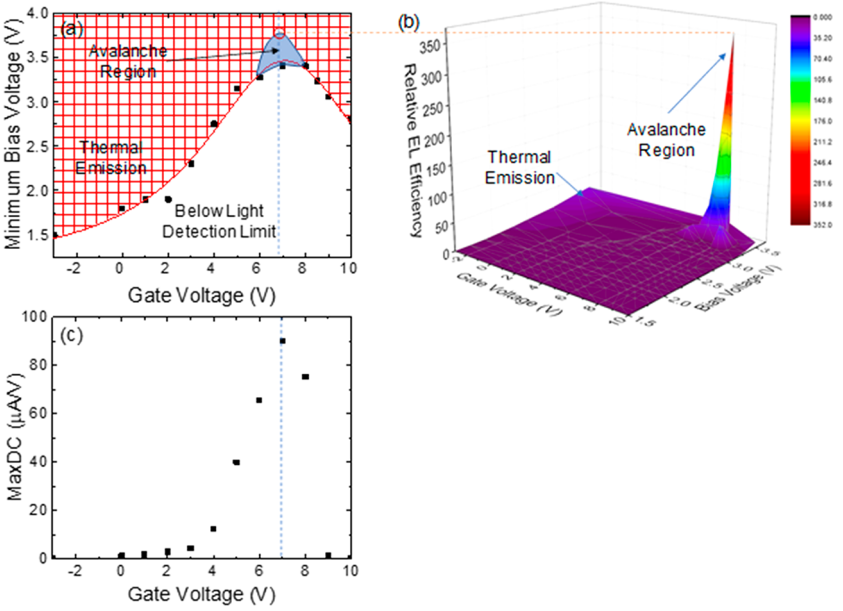

Figure 3. (a) Minimum bias voltage at which light emission is observed plotted as a function of gate voltage. Three regions are labeled on the plot: avalanche region, thermal emission, and below light detection limit. (b) 3D plot of the relative EL efficiency plotted as a function of applied gate and bias voltages. (c) Plot of the maximum differential conductance at different values of gate voltage. This data set was measured at the same time as the data in Figure 2 from the same CNTFET device.

DOI: 10.1021/acsphotonics.8b00896
ACS Photonics XXXX, XXX, XXX−XXX

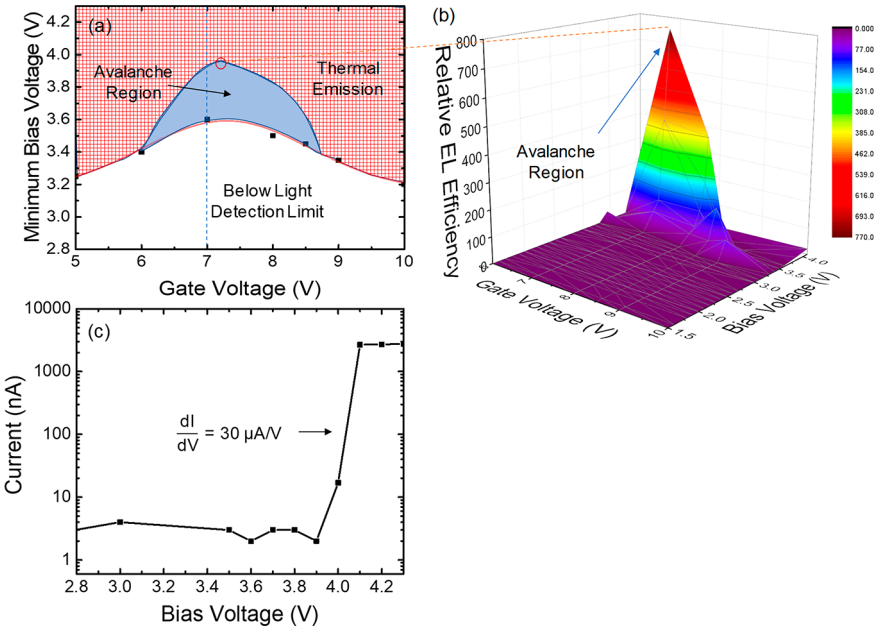

Figure 4. (a) Minimum bias voltage at which light emission is observed plotted as a function of a narrower range of gate voltage. Three regions are labeled on the plot: avalanche region, thermal emission, and below light detection limit. (b) 3D plot of the relative EL efficiency plotted as a function of applied gate and bias voltages. (c) Semi-log plot of the electric current plotted as a function of applied bias voltage at a gate potential of V_g = +7 V.

which has the highest light emission onset voltage, the highest electroluminescence efficiency, and the largest maximum differential conductance.

Figure 4 shows similar data from another CNT FET device. Figure 4a shows the minimum bias voltage needed to reach the light detection limit plotted as a function of gate voltage over a relative narrow range (5−10 V). This data also shows a "triangular" avalanche light emission region and a shaded thermal emission region. Beyond the avalanche light emission region, the current increases abruptly, as shown in Figure 4c, and thermal heating becomes the dominant mechanism of emission. Figure 4b shows a 3D plot of the relative electroluminescence efficiency plotted as a function of the gate voltage and bias voltage, in which another sharp peak appears corresponding to avalanche emission. Figure 4c shows a log plot of the electric current vs applied bias voltage at a gate potential of V_g = +7 V for this FET device, exhibiting a steep current jump with a large differential conductance of 30 μA/V.

These results provide new mechanistic insight regarding light emission in carbon nanotubes that extend beyond our previous work.[12] Here, we have identified a regime of sub-avalanche light emission that we were previously unable to resolve. In addition, we have provided a detailed map of the light emission as a function of the bias and gate voltages, which exhibits a sharp singularity in the electroluminescence efficiency as a function of these variables. This singularity exemplifies how stringent the conditions required are to observe avalanche and sub-avalanche emission (drops off by 2−3 orders of magnitude over just 0.1 V)

In conclusion, in mapping out the electrical bias and gate conditions for light emission in suspended carbon nanotubes, a narrow region occurs corresponding to avalanche breakdown which appears with extremely low current (<5 nA) and electrical powers (<20 nW). Here, we find a sweet spot with the highest electroluminescence efficiency, the highest light emission onset voltage, and the largest maximum differential conductance occurring under the same gate and bias voltage conditions, which provides solid evidence for the avalanche emission mechanism. We also observe efficient light emission below the threshold bias voltage of avalanche emission (i.e., sub-avalanche light emission) by impact ionization. Above the threshold for avalanche breakdown, the electroluminescence efficiency quickly decreases by 2−3 orders of magnitude, and thermal emission becomes the dominant mechanism of light emission.

■ ASSOCIATED CONTENT

Supporting Information

The Supporting Information is available free of charge on the ACS Publications website at DOI: 10.1021/acsphotonics.8b00896.

Additional experimental data including EL and IR images and 3D plots of EL intensity and electric power as a function of gate and bias voltages (PDF)

■ AUTHOR INFORMATION

Corresponding Author

*E-mail: scronin@usc.edu.

ORCID

Bo Wang: 0000-0001-7089-6672

Sisi Yang: 0000-0003-0352-833X

Notes

The authors declare no competing financial interest.

■ ACKNOWLEDGMENTS

The authors would like to acknowledge support from the Northrop Grumman-Institute of Optical Nanomaterials and Nanophotonics (NG-ION^2) (B.W.). This research was supported by the NSF Award No. 1402906 (S.Y.) and Department of Energy DOE Award No. DE-FG02-07ER46376 (L.S.). A portion of this work was carried out in

DOI: 10.1021/acsphotonics.8b00896
ACS Photonics XXXX, XXX, XXX−XXX

the University of California Santa Barbara (UCSB) nanofabrication facility.

REFERENCES

(1) Matsunaga, R.; Matsuda, K.; Kanemitsu, Y. Observation of Charged Excitons in Hole-Doped Carbon Nanotubes Using Photoluminescence and Absorption Spectroscopy. *Phys. Rev. Lett.* **2011**, *106*, 037404.
(2) Yuma, B.; Berciaud, S.; Besbas, J.; Shaver, J.; Santos, S.; Ghosh, S.; Weisman, R. B.; Cognet, L.; Gallart, M.; Ziegler, M.; Honerlage, B.; Lounis, B.; Gilliot, P. Biexciton, single carrier, and trion generation dynamics in single-walled carbon nanotubes. *Phys. Rev. B: Condens. Matter Mater. Phys.* **2013**, *87*, 205412.
(3) Hogele, A.; Galland, C.; Winger, M.; Imamoglu, A. Photon antibunching in the photoluminescence spectra of a single carbon nanotube. *Phys. Rev. Lett.* **2008**, *100*, 217401.
(4) Ma, X. D.; Hartmann, N. F.; Baldwin, J. K. S.; Doorn, S. K.; Htoon, H. Room-temperature single-photon generation from solitary dopants of carbon nanotubes. *Nat. Nanotechnol.* **2015**, *10*, 671−675.
(5) He, X. W.; Hartmann, N. F.; Ma, X. D.; Kim, Y.; Ihly, R.; Blackburn, J. L.; Gao, W. L.; Kono, J.; Yomogida, Y.; Hirano, A.; Tanaka, T.; Kataura, H.; Htoon, H.; Doorn, S. K. Tunable room-temperature single-photon emission at telecom wavelengths from sp(3) defects in carbon nanotubes. *Nat. Photonics* **2017**, *11*, 577.
(6) Mueller, T.; Kinoshita, M.; Steiner, M.; Perebeinos, V.; Bol, A. A.; Farmer, D. B.; Avouris, P. Efficient narrow-band light emission from a single carbon nanotube p-n diode. *Nat. Nanotechnol.* **2010**, *5*, 27−31.
(7) Misewich, J. A.; Martel, R.; Avouris, P.; Tsang, J. C.; Heinze, S.; Tersoff, J. Electrically induced optical emission from a carbon nanotube FET. *Science* **2003**, *300*, 783−786.
(8) Bushmaker, A. W.; Deshpande, V. V.; Bockrath, M. W.; Cronin, S. B. Direct observation of mode selective electron - phonon coupling in suspended carbon nanotubes. *Nano Lett.* **2007**, *7*, 3618−3622.
(9) Hsu, I. K.; Pettes, M. T.; Aykol, M.; Shi, L.; Cronin, S. B. The effect of gas environment on electrical heating in suspended carbon nanotubes. *J. Appl. Phys.* **2010**, *108*, 084307.
(10) Amer, M.; Bushmaker, A.; Cronin, S. Anomalous kink behavior in the current-voltage characteristics of suspended carbon nanotubes. *Nano Res.* **2012**, *5*, 172−180.
(11) Liu, Z. W.; Bushmaker, A.; Aykol, M.; Cronin, S. B. Thermal Emission Spectra from Individual Suspended Carbon Nanotubes. *ACS Nano* **2011**, *5*, 4634−4640.
(12) Wang, B.; Rezaeifar, F.; Chen, J. H.; Yang, S.; Kapadia, R. S.; Cronin, S. B. Avalanche Photoemission in Suspended Carbon Nanotubes: Light without Heat. *ACS Photonics* **2017**, *4*, 2706−2710.
(13) O'Connell, M. J.; Bachilo, S. M.; Huffman, C. B.; Moore, V. C.; Strano, M. S.; Haroz, E. H.; Rialon, K. L.; Boul, P. J.; Noon, W. H.; Kittrell, C.; Ma, J. P.; Hauge, R. H.; Weisman, R. B.; Smalley, R. E. Band gap fluorescence from individual single-walled carbon nanotubes. *Science* **2002**, *297*, 593−596.
(14) Lefebvre, J.; Austing, D. G.; Bond, J.; Finnie, P. Photoluminescence imaging of suspended single-walled carbon nanotubes. *Nano Lett.* **2006**, *6*, 1603−1608.
(15) Chen, J.; Perebeinos, V.; Freitag, M.; Tsang, J.; Fu, Q.; Liu, J.; Avouris, P. Bright infrared emission from electrically induced excitons in carbon nanotubes. *Science* **2005**, *310*, 1171−1174.
(16) Khasminskaya, S.; Pyatkov, F.; Slowik, K.; Ferrari, S.; Kahl, O.; Kovalyuk, V.; Rath, P.; Vetter, A.; Hennrich, F.; Kappes, M. M.; Gol'tsman, G.; Korneev, A.; Rockstuhl, C.; Krupke, R.; Pernice, W. H. P. Fully integrated quantum photonic circuit with an electrically driven light source. *Nat. Photonics* **2016**, *10*, 727.
(17) Mann, D.; Kato, Y. K.; Kinkhabwala, A.; Pop, E.; Cao, J.; Wang, X. R.; Zhang, L.; Wang, Q.; Guo, J.; Dai, H. J. Electrically driven thermal light emission from individual single-walled carbon nanotubes. *Nat. Nanotechnol.* **2007**, *2*, 33−38.
(18) Xie, L. M.; Farhat, H.; Son, H. B.; Zhang, J.; Dresselhaus, M. S.; Kong, J.; Liu, Z. F. Electroluminescence from Suspended and On-Substrate Metallic Single-Walled Carbon Nanotubes. *Nano Lett.* **2009**, *9*, 1747−1751.
(19) Wang, S.; Zeng, Q. S.; Yang, L. J.; Zhang, Z. Y.; Wang, Z. X.; Pei, T. A.; Ding, L.; Liang, X. L.; Gao, M.; Li, Y.; Peng, L. M. High-Performance Carbon Nanotube Light-Emitting Diodes with Asymmetric Contacts. *Nano Lett.* **2011**, *11*, 23−29.
(20) Xie, X.; Islam, A. E.; Wahab, M. A.; Ye, L. N.; Ho, X. N.; Alam, M. A.; Rogers, J. A. Electroluminescence in Aligned Arrays of Single-Wall Carbon Nanotubes with Asymmetric Contacts. *ACS Nano* **2012**, *6*, 7981−7988.
(21) Jakubka, F.; Grimm, S. B.; Zakharko, Y.; Gannott, F.; Zaumseil, J. Trion Electroluminescence from Semiconducting Carbon Nanotubes. *ACS Nano* **2014**, *8*, 8477−8486.
(22) Higashide, N.; Yoshida, M.; Uda, T.; Ishii, A.; Kato, Y. K. Cold exciton electroluminescence from air-suspended carbon nanotube split-gate devices. *Appl. Phys. Lett.* **2017**, *110*, 191101.
(23) Deshpande, V. V.; Hsieh, S.; Bushmaker, A. W.; Bockrath, M.; Cronin, S. B. Spatially Resolved Temperature Measurements of Electrically Heated Carbon Nanotubes. *Phys. Rev. Lett.* **2009**, *102*, 105501.
(24) Pop, E.; Mann, D.; Cao, J.; Wang, Q.; Goodson, K. E.; Dai, H. J. Negative differential conductance and hot phonons in suspended nanotube molecular wires. *Phys. Rev. Lett.* **2005**, *95*, 155505.
(25) Bushmaker, A. W.; Deshpande, V. V.; Hsieh, S.; Bockrath, M. W.; Cronin, S. B. Gate Voltage Controllable Non-Equilibrium and Non-Ohmic Behavior in Suspended Carbon Nanotubes. *Nano Lett.* **2009**, *9*, 2862−2866.
(26) Bushmaker, A. W.; Amer, M. R.; Cronin, S. B. Electrical Transport and Channel Length Modulation in Semiconducting Carbon Nanotube Field Effect Transistors. *IEEE Trans. Nanotechnol.* **2014**, *13*, 176−181.
(27) Bushmaker, A. W.; Deshpande, V. V.; Hsieh, S.; Bockrath, M. W.; Cronin, S. B. Direct Observation of Born-Oppenheimer Approximation Breakdown in Carbon Nanotubes. *Nano Lett.* **2009**, *9*, 607−611.
(28) Bushmaker, A. W.; Deshpande, V. V.; Hsieh, S.; Bockrath, M. W.; Cronin, S. B. Large Modulations in the Intensity of Raman-Scattered Light from Pristine Carbon Nanotubes. *Phys. Rev. Lett.* **2009**, *103*, 067401.
(29) Chang, S. W.; Theiss, J.; Hazra, J.; Aykol, M.; Kapadia, R.; Cronin, S. B. Photocurrent spectroscopy of exciton and free particle optical transitions in suspended carbon nanotube pn-junctions. *Appl. Phys. Lett.* **2015**, *107*, 053107.
(30) Deshpande, V. V.; Chandra, B.; Caldwell, R.; Novikov, D. S.; Hone, J.; Bockrath, M. Mott Insulating State in Ultraclean Carbon Nanotubes. *Science* **2009**, *323*, 106−110.

DOI: 10.1021/acsphotonics.8b00896
ACS Photonics XXXX, XXX, XXX−XXX